Cluster observations of broadband electromagnetic waves in and around a reconnection region in the Earth's magnetotail current sheet

P. Petkaki,[1] M. P. Freeman,[1] and A. P. Walsh[1,2]

Received 2 June 2006; revised 7 July 2006; accepted 24 July 2006; published 31 August 2006.

[1] We present an analysis of the electric and magnetic wave spectra on kinetic scales during several crossings of a reconnecting current sheet. The spectra were measured from 1 Hz or less up to 4096 Hz by the EFW, FGM and STAFF instruments onboard the Cluster spacecraft between 3 and 4 UT on 11 October 2001. During the event plasma flows of order of the local Alfvén speed reversed from tailward to earthward, suggesting that a reconnection site moved over the spacecraft. We ordered the observed electric and magnetic field wave spectrum by the position within the current sheet using the magnitude of the magnetic field B. We found that the electric and magnetic wave power decreased considerably at all frequencies towards the center of the current sheet ($B \approx 0$ nT). The electric energy density decreases 5 orders of magnitude from the edge of the current sheet (B = 19 nT) to the center and the magnetic energy density peaks within the current sheet (B = 13 nT) and is decreased by 2.5 orders of magnitude at the center. Within the current sheet, the electric and magnetic wave spectra were dominantly broadband electromagnetic noise (i.e., power law spectra with exponents ≈ -1.4 and ≈ -2.4, respectively) throughout the frequency range $\sim$0.1–1000 Hz, spanning from MHD (i.e., ion cyclotron frequency $\approx$0.2 Hz) to almost the electron plasma frequency ($\approx$4000 Hz). We argue that the wave activity is likely to be whistler wave turbulence and discuss the implications of these results for reconnection from wave-particle interactions.
Citation: Petkaki, P., M. P. Freeman, and A. P. Walsh (2006), Cluster observations of broadband electromagnetic waves in and around a reconnection region in the Earth's magnetotail current sheet, *Geophys. Res. Lett.*, *33*, L16105, doi:10.1029/2006GL027066.

1. Introduction

[2] One of the main scientific contributions of the Cluster spacecraft mission is to the understanding of magnetic reconnection in the Earth's magnetosphere (including magnetopause and magnetotail). In particular, two aims of the Wave Experiment Consortium (WEC) are to characterize plasma waves and turbulence and to assess their role in the 'anomalous' behaviour of thin critical layers where the MHD approximation is broken [*Roux and de la Porte*, 1988].

[3] In collisionless space plasmas such as the Earth's magnetosphere, magnetic reconnection requires the breakdown of the ion and electron frozen-in condition at the magnetic null point. Possible breakdown mechanisms include anomalous resistivity from wave-particle interactions involving the lower hybrid drift instability (LHDI) [*Huba et al.*, 1977] and the ion-acoustic instability (IAI) [*Galeev and Sagdeev*, 1984; *Watt et al.*, 2002; *Hellinger et al.*, 2004; *Petkaki et al.*, 2003, 2006], drag from Bunemann wave turbulence [*Drake et al.*, 2003], and electron pressure anisotropy [*Birn et al.*, 2001]. Besides their theoretical possibilities, the importance of the wave-associated mechanisms has been highlighted by observations of IA [*Scarf et al.*, 1984], LH [*Bale et al.*, 2002; *Carter et al.*, 2002], upper hybrid [*Farrell et al.*, 2002] and whistler [*Deng and Matsumoto*, 2001] waves associated with reconnection in space and laboratory plasmas. Some wave modes like LH waves and whistler mode waves require the presence of a magnetic field, while others like IA waves can be excited at magnetic null points or neutral sheets. Thus it is important to establish where the observed waves occur within the current sheet and whether they actually cause the breakdown of the ion or electron frozen-in condition or merely arise from the reconnection process.

[4] In this paper we present an analysis of observations of the Earth's magnetotail by the four Cluster spacecraft at 3–4 UT, October 11 2001, in order to investigate how wave activity is related to position in a reconnecting current sheet, to identify the dominant wave modes, and to relate observations to simulations of wave-particle interactions.

2. Observations and Analysis

[5] During the interval 03:00–04:00 UT on October 11 2001 Cluster was in the magnetotail and made several crossings of the central current sheet in the pre-midnight sector north of the magnetic equator. The average minimum spacecraft separation was 1752 km and the average maximum separation was 1996 km. The mean position in Geocentric Solar Ecliptic (GSE) coordinates was X = −99695.4 km (15.65 R_e), Y = 69469.3 km (10.9 R_e) and Z = 12300.2 km (1.93 R_e). In this paper we are going to look in detail at the observations from the Cluster spacecraft 1 (SC1), with reference to data from the other three spacecraft where appropriate. Figure 1 presents a summary of the SC1 data, divided by vertical guidelines into five regimes for the convenience of the subsequent description. (We produced similar plots from all four spacecraft where data were available.)

[6] Figure 1c shows the three components of the magnetic field in GSM coordinates from high resolution FGM measurements [*Balogh et al.*, 2001]. Component B_x is shown in blue, B_y in green and B_z in red. Throughout the interval, SC1 was in the central plasma sheet (defined as $\beta \geq 0.5$ [*Angelopoulos et al.*, 1994]) except at $\sim$03:35:40 UT

[1]British Antarctic Survey, Cambridge, UK.
[2]Mullard Space Science Laboratory, Dorking, UK.

0094-8276/06/2006GL027066

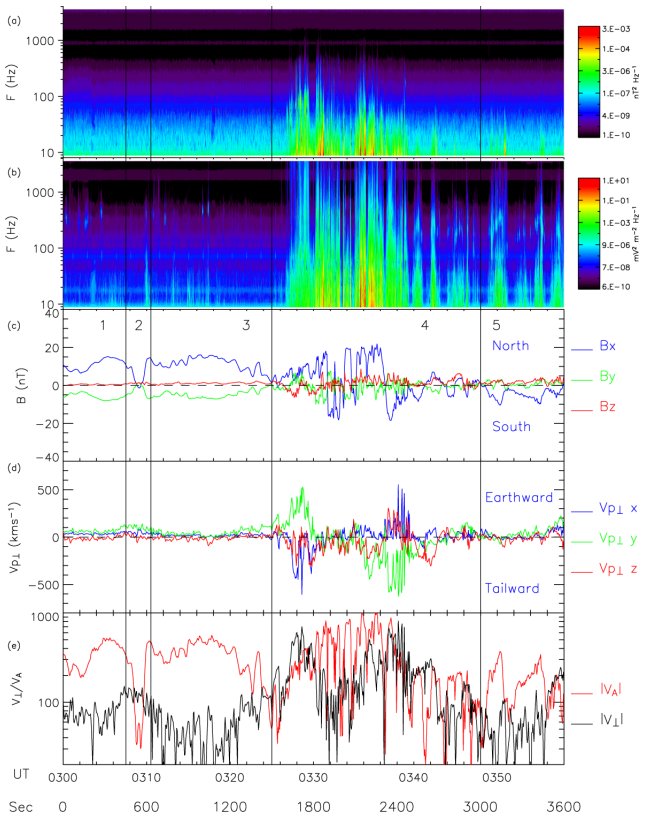

Figure 1. Summary of observations made by the Cluster 1 spacecraft in the interval 03:00–04:00 UT on 11 October 2001. (a) STAFF magnetic field spectra. (b) STAFF electric field spectra. (c) FGM high resolution magnetic field components in GSM coordinates. (d) CIS proton flow velocity components perpendicular to the magnetic field. (e) Perpendicular proton flow speed to Alfvén speed ratio $V_{p\perp}/V_A$.

when it touched the northern lobe (where $B \approx 20$ nT). SC1 moved from the northern half of the current sheet ($B_x > 0$) in regimes 1 and 3 to the southern half ($B_x < 0$) in regime 5, making a transient partial crossing of the current sheet center in regime 2 and several transient partial or complete crossings in regime 4, as indicated by the repeated magnetic reversals of the B_x component. Typically, the magnetic field measured by the other Cluster spacecraft (not shown) had the same sign of B_x as SC1 and hence we deduce that the current sheet thickness was greater than the spacecraft separation. However, at 03:30:25–03:31:40 and 03:35–03:36:40 UT, SC1 and SC3 measured B_x values of opposite polarity and magnitude close to the lobe magnetic field value of 20 nT, implying a current sheet thickness comparable to the spacecraft separation of ~1800 km, and half-thickness similar to the ion inertial length, $c/\omega_{pi} \sim$ 500–1300 km.

[7] Figure 1d shows the three components of the proton flow velocity perpendicular to the magnetic field in GSM coordinates from the CIS-CODIF experiment [*Rème et al.*, 2001]. Proton velocities were calculated from 3D moments of the distribution function. The data were then transformed into the GSM coordinate frame. Velocities perpendicular to the magnetic field were calculated using the formula $V_{p\perp} = \mathbf{B} \times (\mathbf{V}_p \times \mathbf{B})/B^2$ [see *Runov et al.*, 2003]. Component $V_{p_\perp x}$ is shown in blue, $V_{p_\perp y}$ in green and $V_{p_\perp z}$ in red. Typically, the perpendicular flow speed is low, except during regime 4 when high-speed (>100 km/s) flows reversed from primarily tailward (negative $V_{p_\perp x}$) and duskward (positive $V_{p_\perp y}$) to primarily earthward (positive $V_{p_\perp x}$) and dawnward (negative $V_{p_\perp y}$). High-speed flow reversals in the same sense as for SC1 are also seen in the CIS data from SC3 and SC4 (there is no active CIS experiment aboard SC2). This suggests that in regime 4 a reconnection X-line moved over the spacecraft [see, e.g., *Ueno et al.*, 1999] with its normal in the current sheet plane tilted earthward and dawnward.

[8] Further support for reconnection during regime 4 is provided in Figure 1e which compares the $V_{p\perp}$ flow speed with the local Alfvén speed calculated from the magnetic field and density measurements from 3D moments of the proton, He^+, He^{2+} and O^+ distribution functions by CODIF. The flow speed is typically comparable to the Alfvén speed whenever the spacecraft is positioned deep in the current sheet (small magnitude of the magnetic field and low Alfvén speed), consistent with the expectations of reconnection theory [see, e.g., *Priest and Forbes*, 2000].

[9] Figures 1a and 1b show the magnetic and electric field wave spectra, respectively, measured from 8Hz to 4096 Hz by the STAFF instrument [*Cornilleau-Wehrlin et al.*, 1997]. During regime 4, enhanced broadband wave activity is observed that likely extends to frequencies below the minimum frequency measured by STAFF. Consequently, the wave enhancement seems closely associated with the passage over the spacecraft of the high-speed plasma flow reversal and inferred reconnection X-line, especially since there is no significant wave activity prior to regime 4, including during the relatively low-speed partial current sheet crossing in regime 2, and wave activity is also weaker in regime 5 when the flow speed is low and it is inferred that the reconnection X-line has passed downtail or reconnection has ceased.

[10] Although the wave activity during regime 4 is generally enhanced, it is nevertheless bursty. On closer inspection of the data, we noticed that the wave activity appears to reduce every time the background magnetic field strength B measured by FGM reduces and approaches zero. This suggested to us that the wave activity is ordered by the distance of the spacecraft from the center of the current sheet, for which B is a reasonable proxy (e.g., the Harris current sheet [*Harris*, 1962]). To investigate this, Figure 2 shows the magnetic and electric field spectra re-ordered with respect to B rather than time. This was done by sorting the magnetic and electric field wave spectra measured by STAFF during 03:25–03:42 UT according to B measured by FGM. For each bin $i - 1 < B < i$ nT where $i = 1, 2, 3, \ldots$, an average was calculated of all the spectra observed while B was in that range. Thus we find the average spectrum for all occasions. The re-ordered spectra confirm that wave power is reduced in the center of the current sheet ($B < 1$ nT) and maximizes towards the lobes ($B \approx 20$ nT). Specifically, the electric energy density integrated over the STAFF frequency range is a minimum of 5.9×10^{-22} J m^{-3} at $B < 1$ nT and a maximum of 6.9×10^{-17} J m^{-3} at $B = 19$ nT (within a broad plateau between 15 and 21 nT). The magnetic energy density is a minimum of 3.1×10^{-18} J m^{-3} at $B < 1$ nT and a maximum of 7.4×10^{-16} J m^{-3} at $B = 13$ nT (within a broad

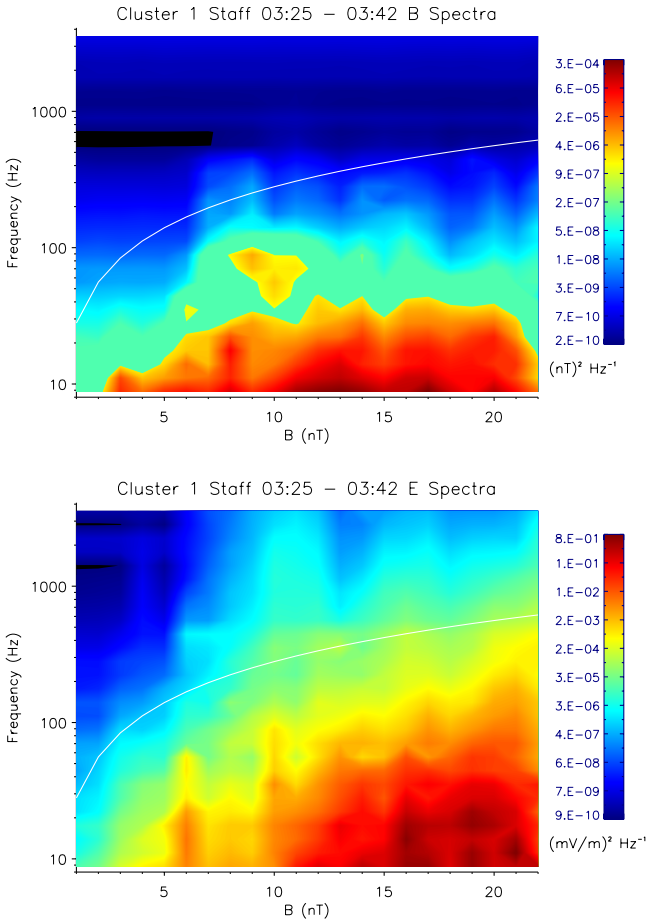

Figure 2. (top) Magnetic field spectra re-ordered with respect to magnitude of the magnetic field B during 03:25–03:42 UT. (bottom) Electric field spectra re-ordered as the magnetic field spectra. For reference, the white curve shows the electron cyclotron frequency ($f_{ce} \approx 28\ B$ [nT]).

plateau between 10 and 20 nT). Similar spectra and levels of wave activity are seen on the other spacecraft.

[11] The re-ordered spectra are broadband and appear to be relatively unstructured, except for a peak at a few tens of Hz in the magnetic field wave spectrum. This indicates a turbulent cascade extending to frequencies outside those measured by the STAFF instrument. To investigate this, we calculated electric and magnetic power spectra over an extended frequency range by adding electric field data at a resolution of 25 vectors/second from the EFW instrument (high-pass filtered with a 2 Hz cut-off) [*Gustafsson et al.*, 2001] and magnetic field data at a resolution of 22.3 vectors/second from the FGM instrument for a time interval 03:28:57 to 03:29:17 UT (1737–1757 seconds after 03 UT) during which the magnetic field was relatively stable ($10 \leq B \leq 12$ nT) and corresponding to a location within the current sheet. The EFW/FGM range of frequencies is from ~0.04 Hz to ~12 Hz so it overlaps with the STAFF spectra (8 Hz to 4096 Hz). We fast Fourier transformed the EFW and FGM data to produce the power spectra at low frequencies and time averaged the STAFF electric and magnetic field spectra over the time interval to yield the spectra at high frequencies. In Figure 3 we plot the resultant energy density spectrum. The two corresponding low and high frequency spectra match at the common frequencies, giving confidence in the instrument calibrations. (The flattening of the magnetic field wave spectrum between 5 and 12 Hz is due to the wave power falling below the instrument noise threshold.) Overplotted are several linear wave frequencies - the electron and ion cyclotron frequencies f_{ce} and f_{ci}, the lower hybrid frequency $f_{LH} = (f_{ce}\, f_{ci})^{1/2}$) for an electron-proton plasma and the lower hybrid frequency $f_{LHO^+} = (f_{ce} f_{cO^+})^{1/2}$) for an electron-oxygen plasma, the electron and proton plasma frequencies f_{pe} and f_{pp}, and the ion-acoustic frequencies f_{IA} in their likely unstable range $0.3 < k\,\lambda_{De} < 0.6$ (λ_{De} is the Debye length). Variation in the individual frequencies reflects variation of B or density during the interval. The magnetic field spectrum comprises two components - a broadband power-law component from 0.1 to 1000 Hz with exponent ≈−2.4 (black solid line) and a narrowband component peaking close to $f_{pp} \approx 95$ Hz. Similarly, the electric field spectra comprises a broadband power-law component from 1 to 1000 Hz with exponent ≈−1.4 and a superposed narrowband enhancement peaking close to f_{pp}, plus an additional narrowband component at ≈400 Hz, just above f_{ce}. Comparing energy densities, the wave activity is electromagnetic in the range of ~1 Hz to ~1 kHz.

3. Discussion and Summary

[12] We have analyzed the electric and magnetic wave fields measured by Cluster during an event in which the

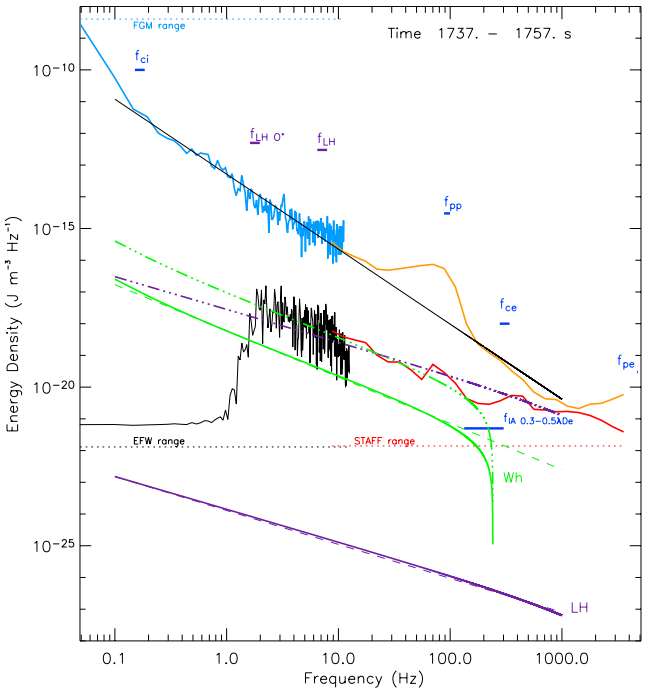

Figure 3. Magnetic field energy density spectrum from FGM (blue) and STAFF (orange) and electric field spectrum from EFW (black) and STAFF (red) from SC1 for the interval 03:28:57 to 03:29:17 UT. Approximate power law fit to the magnetic field spectrum (black). Predicted electric field spectrum based on LH waves (solid purple), approximate power law fit (dashed purple), and shifted predicted spectrum (dot-dashed purple). Similarly for whistler waves (solid, dashed and dot-dashed green).

spacecraft made multiple crossings through the magnetotail current sheet and observed strong earthward and tailward flows at Alfvénic speeds, indicative of the bi-directional jets of a magnetic reconnection region. Wave-particle interactions have been proposed as a mechanism for the breakdown of the ion and electron frozen-in condition that is necessary for magnetic reconnection to occur in the collisionless plasma of the magnetotail. The aim of the study has been to elucidate the general relationship between waves and reconnection by examining (a) when, (b) where and (c) what type of waves occur with respect to reconnection.

[13] (a) From Figure 1, we found that broadband electric and magnetic wave activities are enhanced in those current sheet crossings that have high-speed flows and are inferred to be close to an active reconnection site. Previous observations have also reported that the intensity and the frequency of occurrence of broadband electrostatic noise [*Anderson*, 1984] and whistler waves [*Deng and Matsumoto*, 2001] increase in the presence of strong plasma flows in the magnetotail and the magnetopause current sheet, respectively.

[14] (b) From Figure 2, the emission power appears to be strongly ordered by the position in the magnetotail current sheet, and is heavily reduced in the centre of the current sheet where the breakdown of the electron frozen-in condition would occur. *Bale et al.* [2002] report a similar wave power reduction towards the center of the magnetopause current sheet. In our case, the electric energy density decreases 5 orders of magnitude from the outer edge of the current sheet ($15 < B < 21$ nT) to the center ($B < 1$ nT). The magnetic energy density decreases by 2 orders of magnitude from the outer region of the current sheet ($B >$ 10 nT) to the center. Wave power still exists at the current sheet centre - the magnetic and electric energy densities integrated over the STAFF frequency range are 3.1×10^{-18} J m^{-3} and 5.9×10^{-22} J m^{-3}, respectively. It is an interesting challenge to theory or simulation to ask whether this wave power is sufficient to cause enough anomalous resistivity to break down the electron frozen-in condition and thereby allow reconnection to occur by wave-particle interactions.

[15] (c) Plasma waves considered as important in the ion and electron diffusion regions have included the IA, LH and whistler (see Introduction). Typically, the STAFF electric and magnetic field spectra show predominantly broadband electromagnetic emissions throughout the current sheet (Figure 2). We examined closely an interval towards the current sheet edge (moderate values of B) shown in Figure 3, where we plotted the electric and magnetic field spectra over 4 orders of magnitude in frequency combining measurements from the EFW, FGM and STAFF instruments. The wave activity is electromagnetic throughout the frequency range spanning from the ion cyclotron frequency (MHD) to almost the electron plasma frequency. The electric and magnetic spectra can both be decomposed into two components - a broadband power law and relatively narrowband peaks. The broadband power law has exponents $a_B \approx -2.4$ and $a_E \approx -1.4$ in the magnetic and electric field spectra, respectively.

[16] Simulations have shown that the IAI can generate significant anomalous resistivity in a current sheet of sufficient current density, but we are aware of only one observation of possible IAI activity in the magnetotail [*Scarf et al.*, 1984]. Here, we observe no clear evidence of a peak in the electric field wave spectra in the range of unstable IA wave frequencies expected for the observed plasma conditions. Two small peaks in the electric field wave spectrum are seen but are not co-located with the maximum growth rate frequency. In addition, the broadband wave spectrum is electromagnetic, inconsistent with IA waves.

[17] Observations at the magnetopause, in the magnetotail and in laboratory experiments have claimed evidence of LH waves associated with reconnection. Simulations of the LHDI show that the wave power is suppressed towards the center of a current sheet, qualitatively similar to the behaviour seen in this study [e.g., *Daughton et al.*, 2004]. However, we find no evidence of an enhancement of wave power at the LH frequency, even close to the region of the current sheet with peak wave power (see Figure 3). The electric field power law exponent of $a_E \approx -1.4$ is larger than the value $a_E \approx -1.0$ obtained by *Bale et al.* [2002] in the Hall current region of the magnetopause, which they attributed to LH waves. In order to test whether the broadband electromagnetic spectrum is consistent with LH waves, we compare whether the relationship between electric and magnetic spectra is consistent with theory. Taking the Fourier transform of Faraday's law, we have that $\omega\tilde{\mathbf{B}} = \mathbf{k} \times \tilde{\mathbf{E}}$, where $\tilde{X}$ denotes the Fourier transform of X. Squaring, we get $\omega^2 |\tilde{\mathbf{B}}|^2 = k^2 |\tilde{\mathbf{E}}|^2$ (assuming $\mathbf{k}.\tilde{\mathbf{E}} = 0$). Substituting for $k(\omega)$ from the linear LH dispersion relation for finite plasma beta and electron temperature less than the ion temperature [*Davidson et al.*, 1977], appropriate to the magnetotail, and approximating the magnetic field power spectrum by a power law with exponent $a_B = -2.36$ (solid black line), we predict the electric field spectrum shown by the solid purple line. The energy density is almost 7 orders of magnitude lower than observed. The spectral slope is close to unity (dashed purple line) which is similar to that observed by *Bale et al.* [2002] but different to $a_E \approx -1.4$ of the observed spectrum (compare with dot-dash purple line which shows predicted LH spectrum shifted up to approximately match the observed energy density). Thus we conclude that the observed spectrum is unlikely to be due to LH waves.

[18] Observations at the magnetopause have also reported evidence for whistler waves associated with fast plasma flows. Similar enhancements are seen here in the whistler frequency range for high beta plasma, i.e, below the electron cyclotron frequency. The narrowband peak is seen in the range 20–140 Hz, similar to the proton plasma frequency. This coincides with the frequency of obliquely propagating whistler waves in the small wavelength limit, as also deduced by *Deng and Matsumoto* [2001]. Regarding the broadband spectral component, for whistler waves in a high beta plasma, we have $\omega \sim k^2$ and hence for a given angle between k and $\tilde{E}$, we find $|\tilde{B}|^2 \sim |\tilde{E}|^2/\omega$, consistent with the observed difference $a_B - a_E = 1$ in the power law spectral slopes. Similarly to the LH case, the solid green curve shows the predicted electric field spectrum based on the power law approximation to the magnetic field spectrum and the full linear whistler dispersion relation for high plasma beta and propagation parallel to the magnetic field [e.g., *Biskamp*, 2000, chapter 6.2]. The energy density is approximately an order of magnitude too low but the

spectral slope of ≈ -1.4 is consistent with the observed spectrum (see dot-dash green line). This suggests that both the broadband power law and narrowband peak of the spectra are likely associated with whistler waves.

[19] In summary, our study has shown that the wave environment of a reconnecting current sheet is likely characterized by non-linear whistler wave turbulence whose power maximises in the high-speed outflow jets close to the X-line and towards the edge of the current sheet.

[20] **Acknowledgments.** We thank A. Buckley, E. Lucek, C. Owen, A. Fazakerley, G. Abel, and R. Horne for useful discussions. We thank N. Cornilleau-Wehrlin, M. Maksimovic, L. Mirioni (STAFF), E. Lucek (FGM), H. Rème, I. Dandouras (CIS-CODIF), M. Andrè, A. Vaivads (EFW) and the Cluster Active Archive for providing the data and associated support.

References

Anderson, R. R. (1984), Plasma waves at and near the neutral sheet, in *ESA Achievements of the International Magnetospheric Study*, *Eur. Space Agency Spec. Publ.*, *ESA SP-217*, 199–204.

Angelopoulos, V., C. F. Kennel, F. V. Coroniti, R. Pellat, M. G. Kivelson, R. J. Walker, C. T. Russell, W. Baumjohann, W. C. Feldman, and J. T. Gosling (1994), Statistical characteristics of bursty bulk flow events, *J. Geophys. Res.*, *97*, 21,257–21,280.

Bale, S. D., F. S. Mozer, and T. Phan (2002), Observation of lower hybrid drift instability in the diffusion region at a reconnecting magnetopause, *Geophys. Res. Lett.*, *29*(24), 2180, doi:10.1029/2002GL016113.

Balogh, A., et al. (2001), The Cluster magnetic field investigation: Overview of in-flight performance and initial results, *Ann. Geophys.*, *19*, 1207–1217.

Birn, J., et al. (2001), Geospace Environment Modeling (GEM) magnetic reconnection challenge, *J. Geophys. Res.*, *106*, 3715–3719.

Biskamp, D. (2000), *Magnetic Reconnection in Plasmas*, Cambridge Univ. Press, New York.

Carter, T. A., et al. (2002), Measurement of lower-hybrid drift turbulence in a reconnecting current sheet, *Phys. Rev. Lett.*, *88*, 015001.

Cornilleau-Wehrlin, N., et al. (1997), The Cluster Spatio-Temporal Analysis of Field Fluctuations (STAFF) experiment, *Space Sci. Rev.*, *79*, 107–136.

Daughton, W., G. Lapenta, and P. Ricci (2004), Nonlinear evolution of the lower-hybrid drift instability in a current sheet, *Phys. Rev. Lett.*, *93*, 105004.

Davidson, R. C., N. T. Gladd, and C. S. Wu (1977), Effects of finite plasma beta on the lower-hybrid-drift instability, *Phys. Fluids*, *20*, 301–310.

Deng, X. H., and H. Matsumoto (2001), Rapid magnetic reconnection in the Earth's magnetosphere mediated by whistler waves, *Nature*, *410*, 557–560.

Drake, J. F., et al. (2003), Formation of electron holes and particle energization during magnetic reconnection, *Science*, *299*, 873–877.

Farrell, W. M., M. D. Desch, M. L. Kaiser, and K. Goetz (2002), The dominance of electron plasma waves near a reconnection X-line region, *Geophys. Res. Lett.*, *29*(19), 1902, doi:10.1029/2002GL014662.

Galeev, A. A., and R. Z. Sagdeev (1984), Current instabilities and anomalous resistivity of plasmas, in *Basic Plasma Physics*, vol. 2, edited by A. A. Galeev and R. N. Sudan, pp. 271–303, Elsevier, New York.

Gustafsson, G., et al. (2001), First results of electric field and density observations by Cluster EFW based on initial months of operation, *Ann. Geophys.*, *19*, 1219–1240.

Harris, E. G. (1962), On a plasma sheath separating regions of oppositely directed magnetic field, *Nuovo Cimento*, *23*, 115–121.

Hellinger, P., P. Trávníček, and J. D. Menietti (2004), Effective collision frequency due to ion-acoustic instability: Theory and simulations, *Geophys. Res. Lett.*, *31*, L10806, doi:10.1029/2004GL020028.

Huba, J. D., N. T. Gladd, and K. Papadopoulos (1977), The lower-hybrid-drift instability as a source of anomalous resistivity for magnetic field line reconnection, *Geophys. Res. Lett.*, *4*, 125–126.

Petkaki, P., C. E. J. Watt, R. B. Horne, and M. P. Freeman (2003), Anomalous resistivity in non-Maxwellian plasmas, *J. Geophys. Res.*, *108*(A12), 1442, doi:10.1029/2003JA010092.

Petkaki, P., M. P. Freeman, T. Kirk, C. E. J. Watt, and R. B. Horne (2006), Anomalous resistivity and the nonlinear evolution of the ion-acoustic instability, *J. Geophys. Res.*, *111*, A01205, doi:10.1029/2004JA010793.

Priest, E., and T. Forbes (2000), *Magnetic Reconnection*, Cambridge Univ. Press, New York.

Rème, H., et al. (2001), First multispacecraft ion measurements in and near the Earth's magnetosphere with the identical Cluster ion spectrometry (CIS) experiment, *Ann. Geophys.*, *19*, 1303–1354.

Roux, A., and B. de la Porte (1988), Wave experiment consortium, in *The Cluster Mission: Scientific and Technical Aspects of the Instruments*, edited by R. Schmidt and T. D. Guyennep, *Eur. Space Agency Spec. Publ.*, *ESA 0379-6566*, 21–23.

Runov, A., et al. (2003), Current sheet structure near magnetic X-line observed by Cluster, *Geophys. Res. Lett.*, *30*(11), 1579, doi:10.1029/2002GL016730.

Scarf, F. L., et al. (1984), Plasma wave spectra near slow mode shocks in the distant magnetotail, *Geophys. Res. Lett.*, *11*, 1050–1053.

Ueno, G., et al. (1999), Distribution of X-type magnetic neutral lines in the magnetotail with Geotail observations, *Geophys. Res. Lett.*, *26*, 3341–3344.

Watt, C. E. J., R. B. Horne, and M. P. Freeman (2002), Ion-acoustic resistivity in plasmas with similar ion and electron temperatures, *Geophys. Res. Lett.*, *29*(1), 1004, doi:10.1029/2001GL013451.

M. P. Freeman, P. Petkaki, and A. P. Walsh, British Antarctic Survey, High Cross, Madingley Road, Cambridge CB3 0ET, UK. (ppe@bas.ac.uk)